

## Sodium fast reactor power monitoring using $^{20}\text{F}$ tagging agent

R. Coulon<sup>†</sup>, S. Normand<sup>†</sup>, G. Ban<sup>\*</sup>, V. Dumarcher<sup>~</sup>, HP. Brau<sup>~</sup>, L. Barbot<sup>†</sup>, T. Domenech<sup>†</sup>, V. Kondrasovs<sup>†</sup>,  
G. Corre<sup>†</sup>, AM. Frelin<sup>†</sup>, T. Montagu<sup>#</sup>, T. Dautremer<sup>#</sup>, E. Barat<sup>#</sup>.

<sup>†</sup> CEA, LIST, Laboratoire Capteurs et Architectures Electroniques  
Centre de Saclay. Bat 516. PC72. 91191 Gif sur Yvette Cedex  
Tel : +33(0)16908252 , Fax: +33(0)169087819 , Email: romain.coulon@cea.fr

<sup>\*</sup> ENSICAEN  
F-14050 Caen, France.

<sup>~</sup> CEA, Marcoule, Groupe Essais Statistiques  
F-30207 Bagnols sur Cèze, France.

<sup>#</sup> CEA, LIST, Laboratoire Processus Stochastiques et Spectres  
Centre de Saclay. Bat 516. PC72. 91191 Gif sur Yvette Cedex

**Abstract** – *This work deals with the use of gamma spectrometry to monitor the fourth generation of sodium fast reactor (SFR) power. Simulation part has shown that power monitoring in short response time and with good accuracy is possible measuring liquid sodium delayed gamma emitters produced in-core. An experimental test is under preparation at French SFR Phénix experimental reactor to validate simulation studies.*

*Physical calculations have been done to correlate gamma activity to the released thermal power. Gamma emitter production rate in the reactor core was calculated with technical and nuclear data as sodium velocity, atomic densities, neutron spectra and incident neutron cross-sections of reactions producing gamma emitters.*

*Then, a thermal hydraulic transfer function was used for taking into account primary sodium flow in our calculations and gamma spectra were determined by Monte-Carlo simulations.*

*For power monitoring problematic, use of a short decay period gamma emitter will allowed to obtain a very fast response system without cumulative and flow distortion effects.*

*The experiment will be set during the reactor “end of life testing”. The Delayed Neutron Detection (DND) system cell has been chosen as the best available primary sodium sample for gamma power monitoring on Phénix reactor due to its short transit time from reactor core to measurement sample and homogenized sampling in the reactor hot pool.*

*The main gamma spectrometer is composed of a coaxial high purity germanium diode (HPGe) coupled with a transistor reset preamplifier. The signal will be then processed by a digital signal processing system (called Adonis) which is optimum for high count rate and various time activity measurements. To limit statistical problems of the signal, an analytical pileup correction method using duration variable given by our spectrometry system (Adonis) and a nonparametric Bayesian inference for photopeak deconvolution will be used.*

### I. INTRODUCTION

The main requirement for power monitoring systems is the ability to measure a large range of power with good accuracy and fast response. On SFR, power is usually measured by heat balance on water to vapour heat exchangers which is correlated with the ex-core neutron

flux measurements. Heat balance power measurement gives the thermal power with a response time about ten minutes. The ex-core neutron power measurement is done by fission chambers (five on Phénix reactor) with several activity ranges settled at the bottom of the primary vessel to cover the entire neutron flux range of more than 11 decades. This measurement instantly estimates the power but it has some

shift problems due to change in chamber fissile nuclei concentration.

Gamma spectrometry systems are not used for this kind of measurement. Although power monitoring using gamma measurement is already used in Pressurised Water Reactors (PWR) by gamma counting measurement using the  $^{16}\text{N}$  tagging agent.

Gamma spectrometry is studying as a power monitoring system for the fourth generation SFR but conventional gamma spectrometry systems are not designed for time varying activity measurement. The Adonis signal processing for gamma spectrometry developed by the CEA-LIST is able to go further through this instrumental limitation<sup>1</sup>.

## II. METHODS

Gamma activity of each radionuclide is linked to reactor parameters as released thermal power, sodium flow rate in the fast neutron flux and other sodium flow data.

In the first part we will introduce the Adonis signal processing system; the second part the primary sodium gamma source term calculations; the third part deals with Phénix experiment and the fourth part gamma spectra simulation on the Phénix experiment.

### II.A. Adonis signal processing for gamma spectrometry

Conventional digital signal processing systems use the same matched filters method as in analogue signal processing. Parameters of this linear filter are adjusted to pre-requirement pulses shape to optimize spectral resolutions and dynamic range. This trapezoidal shaping method gives short range activity abilities. Some pile-up rejection and life time correction methods are settled to increase the dynamic range but they produced shifts on signal measurement above  $6 \times 10^5 \text{ s}^{-1}$  of input count rate.

For time varying activity measurement, loss free counting methods are implemented. Count rates are corrected in real time with instant evaluation of the system dead time but metrological performances of this kind of method are intrinsically limited by the dead time estimation accuracy<sup>2</sup>.

Adonis system has a totally different approach for signal processing using a bimodal Kalman smoother<sup>3</sup>. This nonlinear digital signal processing leads us to take into account the stochastic nature of the pulses arrival. An event stream composed, for each pulse of precise value of energy, duration, and separation with previous event is given. This triplet allows an accurate analysis for time

varying activities and the dynamic range is the largest without setting on a prejudged input signal. The Adonis electronic is shown on Fig. 1.

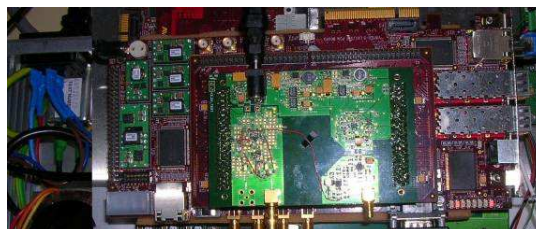


Fig. 1. Adonis electronic

The Fig. 2 shows  $^{241}\text{Am}$  piled-up spectra done with Adonis and commercial Lynx system which is the most advance DSP spectrometry system of Canberra Company. At  $1.3 \times 10^6 \text{ s}^{-1}$ , Adonis gives a less noise spectrum than the Lynx without pile-up rejection using.

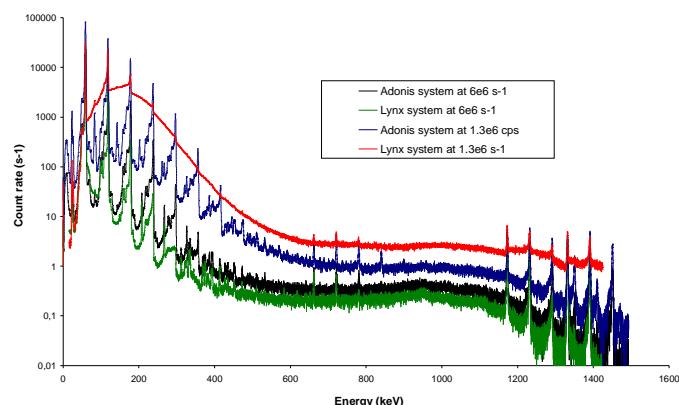


Fig. 2. Adonis and Lynx  $^{241}\text{Am}$  spectra at high count rate

This system is able to provide on-line gamma spectra for input pulse rates from 0 to  $5 \times 10^6 \text{ s}^{-1}$  with still high metrology requirement and optimum spectral resolution (Fig. 3). Furthermore the analytical pileup correction method is only available on Adonis system and is able to remove all spectral the pileup distortion<sup>10</sup>.

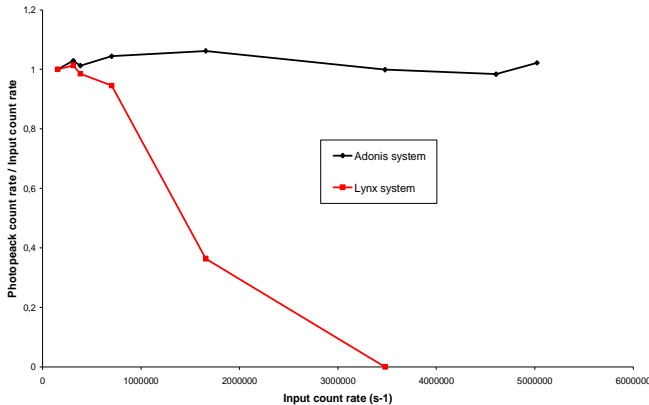


Fig. 3. Adonis and Lynx metrological performance at very high input count rate for 59 keV of gamma energy.

So Adonis system will allow a new application field for on-line gamma spectrometry, as for example reactor monitoring application.

### II.B. SFR primary coolant gamma source term calculation

The gamma source term is calculated as a function of power and sodium flow rate in the fast neutron flux. Equations are an adaptation to SFR from PWR equations developed by B. Papin and P. Bernard<sup>4</sup>. Gamma source terms are calculated with neutron reactions introduced in Table I for each activation radionuclide.

TABLE I  
 Neutron reactions in primary sodium

Nuclear reaction	Induced emitter	Decay period (s)	Photon energy (keV)	Branching ratio
$^{23}\text{Na}(n,2n)$	$^{22}\text{Na}$	$8.22 \times 10^7$	1274.5	1
$^{23}\text{Na}(n,\gamma)$	$^{24}\text{Na}$	$5.39 \times 10^4$	1368.63	1
			2754.03	1
			2870	$2.0 \times 10^{-6}$
			3867.2	$5.2 \times 10^{-4}$
			4238	$7.5 \times 10^{-6}$
$^{23}\text{Na}(n,\gamma)$	$^{24m}\text{Na}$	$2.02 \times 10^{-2}$	472.0	1
$^{23}\text{Na}(n,\alpha)$	$^{20}\text{F}$	$1.10 \times 10^1$	1633.7	1
			3334.4	$1.4 \times 10^{-4}$
			439.9	$3.3 \times 10^{-1}$
$^{23}\text{Na}(n,p)$	$^{23}\text{Ne}$	$3.72 \times 10^1$	1636.4	$1.0 \times 10^{-2}$
			2076.3	$1.0 \times 10^{-3}$
			2542.3	$2.7 \times 10^{-4}$
			2982.2	$3.8 \times 10^{-4}$
			1293.6	1
$^{40}\text{Ar}(n,\gamma)$	$^{41}\text{Ar}$	$6.58 \times 10^3$	1677.0	$5.2 \times 10^{-4}$
			3967.0	$1.5 \times 10^{-5}$

One should notice that the calculation also took into account dissolved argon (concentration of 0.019 ppm) contained into primary sodium<sup>5</sup>.

First, reaction rate is calculated by discrete nuclear data values as shown in Eq. (1):

$$R_j = N_x \sum_E \sigma_j(E) \phi(E) \quad (1)$$

Where:

- $R_j$  is the reaction rate of the reaction number "j".
- $N_x$  is the atomic density of the target nucleus "x" in the homogenized core with non-irradiated fuel (data extracted from technical report<sup>6</sup>).
- $\sigma_j(E)$  is the partial cross section of the reaction number "j" on the nucleus "x". Nuclear data evaluations are used and extracted in logarithmic scale with 100 energy groups by decade (see Fig. 4).

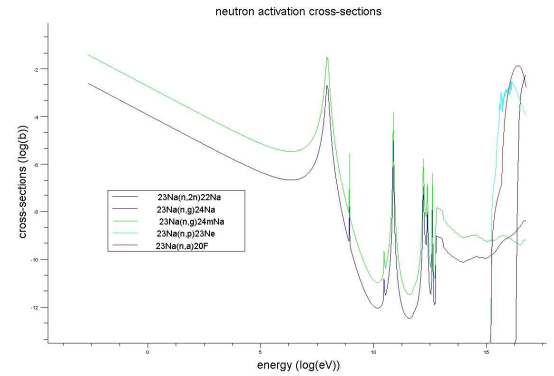


Fig. 4. JEFF 3.1.1 Activation cross-sections of  $^{23}\text{Na}$

- $\Phi(E)$  is the mean neutron Phenix reactor spectrum computed in 33 energy groups using a MCNP5 Neutron transport simulations with a surface flux tally (F4) and homogeneous configuration (Fig. 5 and Fig. 6). The fast neutron velocity induced a high production of threshold reactions as  $^{23}\text{Na}(n,2n)^{22}\text{Na}$ ,  $^{23}\text{Na}(n,p)^{23}\text{Ne}$  and  $^{23}\text{Na}(n,\alpha)^{20}\text{F}$ . Neutron shielding around the core limits ex-core neutron activation (bleu spectrum on Fig. 6).

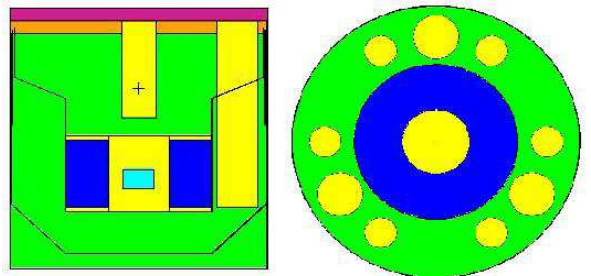


Fig. 5. MCNP5 schematic Phénix primary vessel model

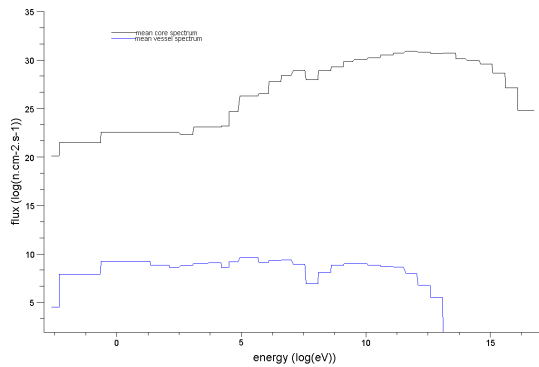


Fig. 6. Phénix neutron spectra at 560 MW

The production rate is then calculated as a function of the thermal power by this formula:

$$X_y = 0.9 \frac{P.R_{act}}{E_f.R_{fiss}.V_c} \quad (2)$$

Where:

- $X_y$  is the production rate producing “y” radionuclide.
- $P$  is the instant thermal power released by the core (the residual power is not include in this value).
- $R_{act}$  is the reaction rate of the reaction creating “y” as activating isotope. We consider only the fissile zone of the core where 90 % of the thermal power is released and where the homogeneous atomic density was calculated. Therefore, a factor is added to compensate this approximation.
- $R_{fiss}$  is the fission rate on  $^{235}\text{U}$  and  $^{239}\text{Pu}$  nucleus calculated using fission cross-sections (Eq. 1 and Fig. 5).
- $E_f$  is the mean energy released per fission.
- $V_c$  is sodium active volume submitted to the fast neutron flux.

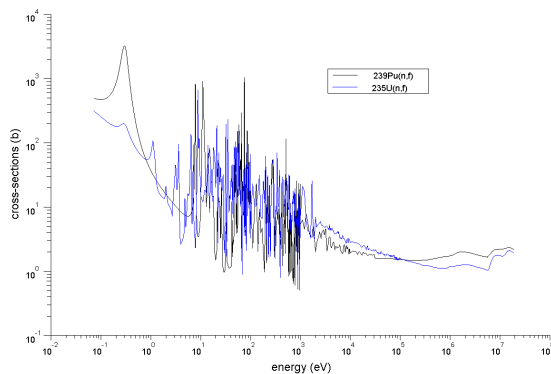


Fig. 7. JEFF 3.1.1 Fission cross-sections on  $^{239}\text{Pu}$  and  $^{235}\text{U}$  nuclei

The activating isotope concentration at the core outlet is obtained by the following differential equation (Eq. 3):

$$\frac{dN_y}{dt} = X_y - (\lambda_y + \alpha) N_y \quad (3)$$

Where:

- $N_y$  is the activating isotope “y” concentration at reactor core outlet.
- $X_y$  is the production rate of the activating isotope “y”.
- $\lambda_y$  is the decay constant of the activating isotope “y”.
- $\alpha$  is a hydraulic parameter which depends of the sodium velocity in active volume. It is calculated as the ratio between sodium flow rate and the sodium active volume of a fuel assembly.

The fuel burn-up is considered as a secondary parameter which changes the fuel enrichment (changing  $R_{fiss}$  parameter in Eq. 2) and control rod position (changing  $V_c$  parameter in Eq.2 and Eq. 3). The sodium temperature is also a second order parameter which induced a nonlinear production rate behaviour (changing  $R_{act}$  parameter in Eq. 2).

During the sodium coolant cycle, radionuclides are diluted in primary coolant and could perform a complete coolant cycle if their decay period is long enough. This effect is neglected for short decay radionuclides as  $^{20}\text{F}$  and  $^{23}\text{Ne}$  but it is predominant for  $^{24}\text{Na}$  and  $^{22}\text{Na}$ . To take into account this cumulative effect, activating isotope concentrations are calculated by adding a cumulative correction as shown in Eq. 4.

$$N'_y = N_y \left( 1 + \sum_{n=1}^{\infty} \int_0^{\infty} \delta_c(t) e^{-n\lambda_y t} dt \right) \quad (4)$$

Where:

- $N'_y$  is the cumulative concentration of the radionuclide “y” at the outlet of fuel assembly.
- $n$  is the coolant cycle number.
- $\delta_c(t)$  is concentration distribution during a coolant cycle.

This cumulative effect increases time to estimate a power value for long period tagging agent. Indeed a short decay period gamma emitter is better to delete this effect and to immediately obtain the power measurement.

### II.C. Phénix experiment

The experimental system will be set during the Phénix reactor “end of life testing”. The Delayed Neutron Detection (DND) cell has been chosen as the best available location on this Phénix reactor (Fig. 9).



Fig. 9. Phénix DND device

This DND system has been set in order to detect clad failure by delayed neutron emitter measurement. This location is optimum for global power measurement due to short sodium transit time (about 30 s) and homogenized measurement done by 6 points in hot pool near each intermediary heat exchanger.

Then, short decay radionuclides measurement and thermal power correlation is potentially achievable.

The main spectrometer is composed of a coaxial high purity germanium (HPGe) diode coupled with a reset transistor preamplifier and a hybrid cryostat (electrical LN2 Cryo-cycle) which is convenient for deported measurement. The HPGe diode signal will be processed by the Adonis signal processing.

The secondary spectrometer is a LaBr3:Ce scintillator coupled with photoelectric electron-multiplier tube. A new numerical electronic coupled with a digital triangular filter will be also implemented. LaBr3:Ce scintillators have the highest resolution of scintillators but it still gives about 2.2 % energy resolution where HPGe diode gives 0.1 % of resolution at the 1.17 MeV <sup>60</sup>Co peak. Despite of its resolution, it will give another measurement of the primary sodium sample with a more gamma dose robust detector.

Detectors are shown in Fig. 10.



Fig. 10. Canberra Cryo-cycle and St-Gobain LaBr3:Ce

### II.D. Gamma spectra simulation on the Phénix experiment

Gamma spectra simulation is divided in two parts. First the thermal hydraulic simulation of the sodium flow between core outlet and measurement sodium sample. Second the gamma transport simulation to finally obtain detector response signal estimation.

Using the Eq. 4, measurement sample concentrations of gamma emitters are calculated by adding a thermal hydraulic correction as shown in Eq. 5.

$$N_y'' = N_y' \sum_{ass=1}^{ass=217} \sum_{ei=1}^{ei=6} \int_0^{\infty} \delta_{ass}^{ei}(t) e^{-\lambda_y t} dt \quad (5)$$

Where:

- $N_y''$  is the concentration of the radionuclide “y” at the measurement point.
- $a_{ss}$  is the fuel assembly number.
- $e_i$  is the intermediate heat exchanger number.
- $\delta(\tau)$  is the hot pool concentration distribution introduced in Eq. 6.

Colchix is a thermal hydraulic model for Phénix reactor. It uses fluorimetry measurements to obtain concentration distribution function at the six intermediate heat exchangers. A typical concentration distribution is shown in the Fig. 11 obtained in Colchix experiments<sup>7</sup>.



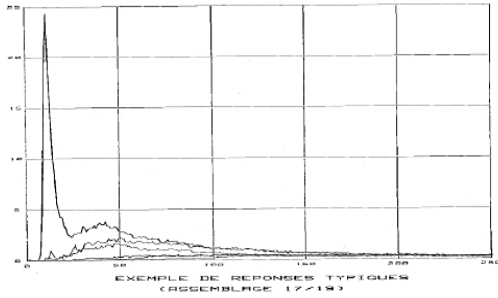


Fig. 11. Typical concentration distribution functions for one fuel assembly outlet

We can notice that sodium flow in the hot pool is very heterogeneous due to the control plug. Sodium has a complex behavior due to the mixture of mixed jet effect, diffusion effect and dilution effect. One of the six responses shows a high jet effect on Fig. 11 which is important to obtain short decay period radionuclides in DND sodium sample. Flow heterogeneities will be corrected by the 6 sodium sample mixture measurement which is essential to obtain global power estimation.

A tridimensional thermal hydraulic simulation project using Trio code is under consideration in collaboration with the thermal hydraulic department of the CEA/DEN to improve the sodium flow distribution knowledge inside Phenix primary hot pool<sup>8</sup>. By convolving a more accurate dilution distribution with radionuclides decay probability, a more precise thermal hydraulic transfer function will be determined.

Thanks to the tagging agent concentration in the DND sample, the incident gamma spectrum is simulated by MCNP5 using a flux point tally (F5) and reduction variance technique due to shield thickness (17 cm of lead around the sodium sample). Fig. 12 is the MCNP model of experiment.

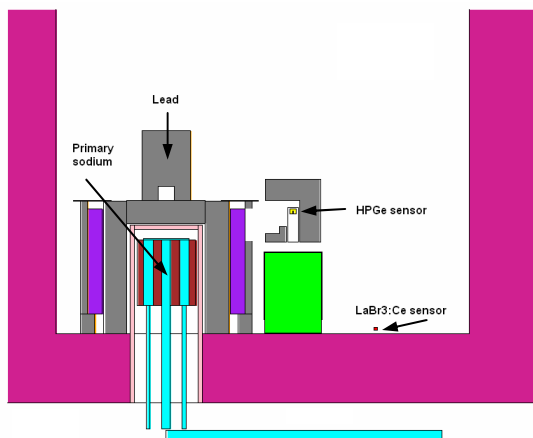


Fig. 12. MCNP model - Phénix experimental test

$$S_e(E) = \eta_e \lambda_y N_y s \sum_{\Delta} \phi_e^{\Delta}(E) V^{\Delta} \quad (8)$$

Where:

- $S_e(E)$  is the incident spectrum on sensor surface due to source photons of energy “e”(listed in Table. 1).
- $\lambda_y$  is the decay constant of the radionuclide “y” producing “e” energy photons.
- $\eta_e$  is the branching ratio of “e” energy photons produced by the radionuclide “y”.
- $N_y$  is the “y” radionuclide concentration in the sodium sample calculated in Eq. 5.
- $s$  is the sensor input surface.
- $\Phi_e^{\Delta}(E)$  is the MCNP5 simulation response for the source photons of “e” energy emitted in the sampling part “ $\Delta$ ” (Fig. 13).
- $V^{\Delta}$  is the volume of the sampling part “ $\Delta$ ”.

To simulate the sensor response, MCNP5 is used with a pulse high tally (F8) in photon-electron mode. Deposited energy during each photon interaction in the sensor is then calculated and finally gives energy deposited spectra by convolving by incident spectra (Eq. 9).

$$S(E) = \sum_e \int_E S_e(E) H(E-e) dE \quad (9)$$

Where:

- $S(E)$  is the response spectrum without noise.
- $S_e(E)$  is the incident spectrum on sensor due to source photons of energy “e”.
- $H(E)$  is efficiency spectra of sensor.

The electronic noise is taken into account by a Gaussian noise convolution on the previews spectrum (Eq. 10).

$$S'(E) = \int_{\epsilon} S(\epsilon) \frac{e^{-\frac{(E-\epsilon)^2}{2\sigma^2(\epsilon, T_{CR})}}}{\sqrt{2\pi\sigma(\epsilon, T_{CR})}} d\epsilon \quad (10)$$

Where:

- $S'(E)$  is the noisy response spectrum.
- $S(E)$  is the deposited energy spectrum.
- $\sigma(E, T_{CR})$  is the resolution parameter of the Gaussian which depends of the pulse energy “E” and the total input count rate “ $T_{CR}$ ” (The resolution evolution as a function of the total input count rate is an Adonis particularity).

In Adonis, piled-up pulses are never rejected. Pile-up contribution is then finally simulated by a recursive calculation using pile-up probability. A summation is done

when a pulse arrives during treatment of a preview pulse (about 350 ns).

### III. RESULTS

This study links reactor power parameters to primary sodium tagging agent concentration which principally depends on the instant released power and the sodium flow rate in the neutron flux.

First part will introduced the Phénix experiment simulation results. Second part will introduced simulation results of an optimum SFR power measurement system.

#### III.A. Simulation results for the Phénix experiment

Experimental Phénix Spectra simulations show the possibility to measure  $^{24}\text{Na}$ , and  $^{20}\text{F}$  tagging agents during our experiment. Our study is then focused on those radionuclides to measure reactor power because  $^{23}\text{Ne}$  exhibits too low photon energy of 440 keV regarding to the DND shielding thickness.

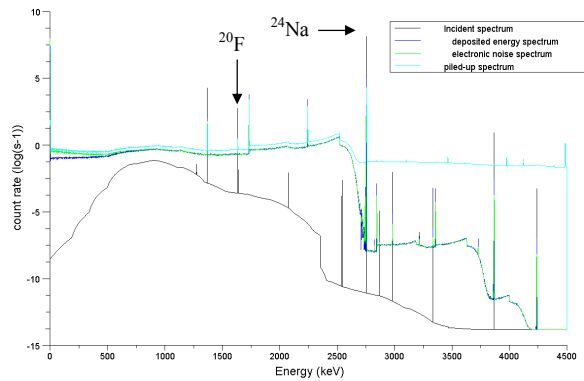


Fig. 19. Simulated mixed gamma spectra of the HPGe signal.

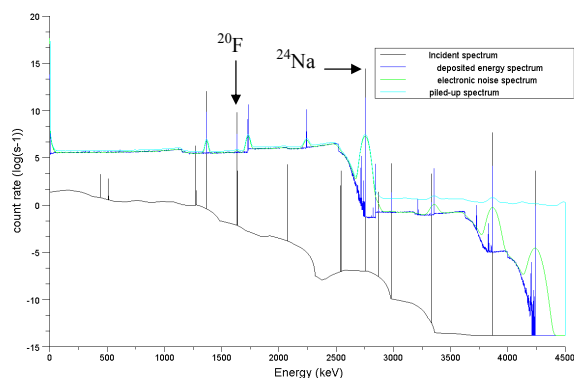


Fig. 20. Simulated mixed gamma spectra of the LaBr3:Ce signal.

The LaBr3:Ce sensor could be settled next to a sodium sample without any lead shielding (see in Fig. 12). The direct to diffuse photon ratio will be better than in the HPGe diode case.

Sodium thermal hydraulic behaviour is the most influent phenomena on the calculation. Simulations are made for 2 extremes cases where the jet effect in the outlet of the assembly is maximal (case 1 in Table 2) and where this effect is minimal (case 2 in Table 2).

TABLE 2

$^{20}\text{F}$  photopeak signal estimation for the Phénix experiment

Detector	case	Signal $^{20}\text{F}$ ( $\text{s}^{-1}$ )	Noise ( $\text{keV}^{-1}.\text{s}^{-1}$ )	Time to exceed detection limit (s)
HPGe	1	1.75	0.70	37.2
	2	0.73	0.56	71.4
LaBr3	1	1873	318	221
	2	643	270	547

This simulation shows the possibility to measure the  $^{20}\text{F}$  gamma activity in the Phénix experiment.

During this experiment, reactor power will be increased by scale of 100 MW to compare at each scale the gamma signal to heat balance power measurement.

In a first time, a relative relation between  $^{20}\text{F}$  activity and reactor power will be obtained.

In a second time, this simulation results will be used as numerical calibration to estimate  $^{20}\text{F}$  nuclei concentration after acquisitions and link it to the power by the Eq. 3.

#### III.B. Simulation results of an optimum SFR power measurement system

The tagging agent core production is directly link to the instant released power but the sodium flow to the measurement cell induced interferences. Sampling has to be done close to the core outlet to limit flow heterogeneity phenomena. Gamma emitters should also have a short decay period (as  $^{20}\text{F}$  and  $^{23}\text{Ne}$ ) to limit flow accumulation phenomena.

To design a power monitoring system measuring short decay period activation products, the transit time from core outlet to measurement sample has to be set as short as possible (Fig. 16).

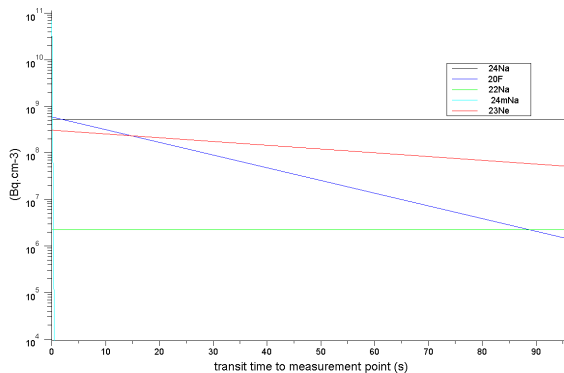


Fig. 16. Tagging agent concentration as a function of transit time to core outlet

This calculation shows that a short time response power monitoring system using  $^{20}\text{F}$  or  $^{23}\text{Ne}$  tagging agent is easily achievable if the sodium sampling volume and the transit time to measurement sample can be designed. Fig. 17 is a spectrum simulated with 2 s of transit time and  $1.5 \times 10^6 \text{ s}^{-1}$  of total incident input count rate.

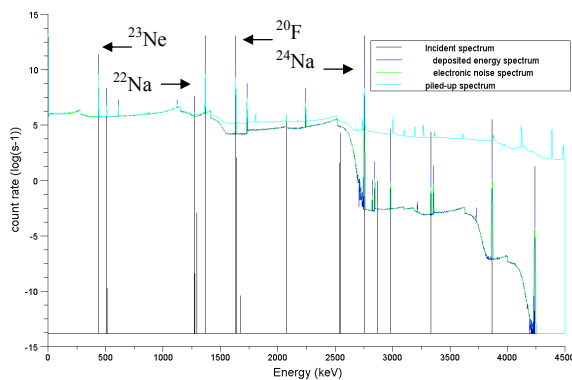


Fig. 17. Simulated mixed gamma spectrum designed for power monitoring system.

TABLE 3

Power dynamic range computed for an Adonis spectrometer

Tagging agents	$^{23}\text{Ne}$	$^{22}\text{Na}$	$^{20}\text{F}$	$^{24}\text{Na}$
Energy (keV)	440	1275	1334	2754
Decay period (s)	$3.72 \times 10^1$	$8.22 \times 10^7$	$1.1 \times 10^1$	$5.39 \times 10^4$
Signal (s-1)	$2.97 \times 10^4$	$6.00 \times 10^2$	$4.14 \times 10^4$	$2.39 \times 10^4$
Noise (keV-1.s-1)	$3.5 \times 10^2$	$4.28 \times 10^2$	$1.97 \times 10^2$	$1.06 \times 10^2$
Dynamic range	$1.2 \times 10^3$	$1.8 \times 10^1$	$1.8 \times 10^3$	$1.3 \times 10^3$

An Adonis system could cover 3 decades of SFR power range. Five systems could cover the entire power range measuring  $^{23}\text{Ne}$ ,  $^{20}\text{F}$  and  $^{24}\text{Na}$  gamma activities.

#### IV. DISCUSSION

This simulation study shows the possibility of  $^{20}\text{F}$  measurement but statistical problem due to pileup effects or too low  $^{20}\text{F}$  detection limits could be met.

Post-processing softwares are developed at CEA-LIST to improve statistics for gamma spectrometry. A new nonparametric Bayesian method is currently designed and used to extract the  $^{20}\text{F}$  signal<sup>9</sup>. In case of piled-up spectra, we will use an analytical pileup correction method using the duration variable given by Adonis<sup>10</sup>.

On-line gamma spectrometry measurement will allow several activation products analysis. This system will permit to design a more autonomous power measurement system with temperature and flow rate correction done only by the gamma spectrometric signal.

#### IV. CONCLUSIONS

This study deals with a new method for power measurement based on sodium activation calculations; thermal hydraulic and gamma photons transport simulations to link gamma signal of primary sodium tagging agents to the released in-core reactor power.

Simulation work has shown that Adonis spectrometry system could be settled as generation IV SFR power monitoring systems matching a large range of power measurement in a short response time.

The Phénix experiment is currently under preparation to validate the method and determine the experimental accuracy of this power measurement system.

#### ACKNOWLEDGMENTS

The authors would like to thank CEA-DRT and CEA-DAM for financial support.

#### REFERENCES

1. J. Morel J. Plagnard and A. Tran Tuan, "Metrological characterization of the Adonis system used in gamma-ray spectrometry," *Applied Radiation and Isotopes*, **60**, 179-183 (2004).
2. ORTEC, "Loss Free Counting with Uncertainty Analysis Using ORTEC's Innovating Zero Dead Time Technique," *Application Note*, AN56.



3. E. Barat T. Dautremer T. Montagu and J. C. Trama, "A Bimodal Kalman Smoother for Nuclear Spectrometry," *Nuclear Instruments and Methods in Physics Research A*, **A567**, 350-352 (2006).
4. B. Papin and P. Bernard, "Mesures de Puissance par Azote 16," *CEA Technical report, SEN n°119*, (1981).
5. J. Devaux and L. Costa, "Activité de l'Argon 41 dans le Ciel de Pile de Phénix," *CEA Technical report, SEDC n°547*, (1974).
6. B. Sicard C. Carnoy and M. Robin, "Données Nécessaires au Calcul Neutronique Simplifié des 3 Premiers Cycles du Cœur Phénix," *CEA Technical report, LSRCY n°2533*, (1979).
7. J. Feraud J. Rion and J. P. Truong, "DND Phénix. Expérience Colchix 1. Analyse de Résultats," *CEA Technical report, LMTE n°5015*, (1989).
8. U. Bieder and E. Graffard, "Qualification of the CFD Code Trio U for Full Scale Reactor Applications," *Nuclear Engineering and Design*, **238**, 671-679 (2008).
9. E. Barat T. Dautremer and T. Montagu, "Nonparametric Bayesian Inference in Nuclear Spectrometry," *Nuclear Science Symposium Conference Record, NSS07*, 880-887 (2007).
10. T. Trigano, "Traitement Statistique du Signal Spectrométrique : Etude du Désempilement de Spectre en Energie pour la Spectrométrie Gamma," *Ph.D. Thesis*, ENST (2005).